



# The ISM in O-star spectroscopic surveys: GOSSS, OWN, IACOB, NoMaDS, and CAFÉ-BEANS

J. Maíz Apellániz

Centro de Astrobiología, CSIC-INTA, ESAC campus, Madrid, Spain  
e-mail: jmaiz@cab.inta-csic.es

**Abstract.** I present results on the interstellar medium towards the O stars observed in five optical spectroscopic surveys: GOSSS, OWN, IACOB, NoMaDS, and CAFÉ-BEANS. I have measured both the amount  $[E(4405 - 5495)]$  and type  $[R_{5495}]$  of extinction towards several hundreds of Galactic O stars and verified that the Maíz Apellániz et al. (2014a) family of extinction laws provides a significantly better fit to optical+NIR Galactic extinction than either the Cardelli et al. (1989) or the Fitzpatrick (1999) families.  $R_{5495}$  values are concentrated between 3.0 and 3.5 but for low values of  $E(4405 - 5495)$  there is a significant population with larger  $R_{5495}$  associated with H II regions. I have also measured different DIBs and I have found that  $W(5797)/W(5780)$  is anticorrelated with  $R_{5495}$ , a sign that extreme  $\zeta$  clouds are characterized not only by low ionization environments (as opposed to  $\sigma$  clouds) but also by having a larger fraction of small dust grains. The equivalent width of the “Gaia DIB” (8621 Å) is strongly correlated with  $E(4405 - 5495)$ , as expected, and its behavior appears to be more  $\sigma$ -like than  $\zeta$ -like. We have also started analyzing some individual sightlines in detail.

**Key words.** Dust, extinction — ISM: lines and bands — Stars: early-type

## 1. O-star spectroscopic surveys

There are several ongoing ground-based optical spectroscopic surveys of early-type stars (mostly of O spectral type but also including B and WR stars) whose main goal is to study the properties of the stars. However, those surveys include large amounts of information on the intervening ISM, which we are also analyzing (Penadés Ordaz et al. 2013; Maíz Apellániz et al. 2014b).

The Galactic O-Star Spectroscopic Survey (GOSSS, Maíz Apellániz et al. 2011) is obtaining blue-violet,  $R \sim 2500$ , high S/N spectroscopy of all O-star candidates that are ac-

cessible to the survey telescopes. Results have already been published in two survey papers (Sota et al. 2011, 2014) and elsewhere (e.g. Walborn et al. 2010, 2011). To date, we have observed and processed 2087 stars and several hundred more have been observed but are still unprocessed. The processed sample includes  $\sim 900$  O stars and  $\sim 900$  B stars up to  $A_V \sim 12$ . The faintest stars are being observed with the 11 m GTC in the north and the 8 m Gemini in the south.

GOSSS is reaching a large number of stars but it is limited by its intermediate resolution, coverage of only the blue-violet region (though some of the spectra reach longer wavelengths),

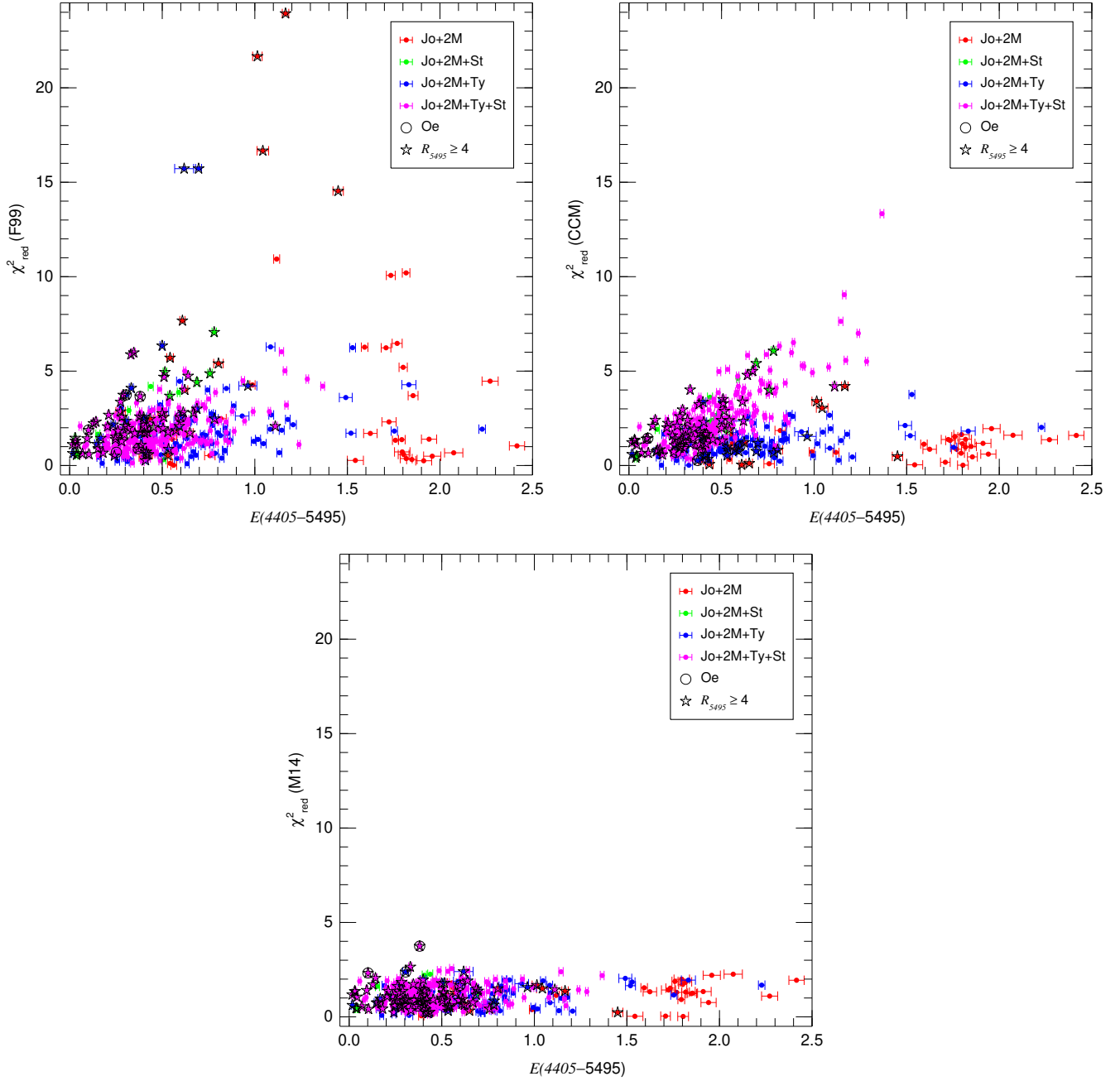


**Fig. 1.**  $\chi^2_{\text{red}}$  of the CHORIZOS fits as a function of  $E(4405 - 5495)$  for the GOSSS I+II sample using the F99 [top left], CCM [top right], and M14 [bottom] families of extinction laws. Note that the vertical scale is the same for the three plots. Different symbols are used for stars with different sets of photometric data (Jo = Johnson, 2M = 2MASS, Ty = Tycho-2, St = Strömgren). Oe stars (which are expected to have poorer fits due to IR excesses) and stars with  $R_{5495} \geq 4$  are marked.

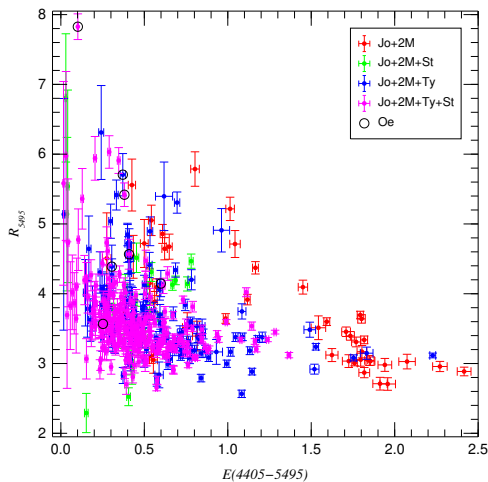


**Fig. 2.**  $R_{5495}$  as a function of  $E(4405 - 5495)$  for the CHORIZOS fits for the GOSSS I+II sample using the M14 family of extinction laws. See Fig. 1 for the symbol nomenclature.

and single-or-few epochs available per star. There are several surveys that complement those limitations by obtaining high-resolution spectroscopy of a subsample of the GOSSS targets. OWN is observing the southern stars using three different telescopes and multiple epochs with the main purpose of studying spectroscopic binarity (Barbá et al. 2010). IACOB and IACOB-sweG are observing northern stars with the main purpose of characterizing their properties (Simón-Díaz et al. 2011). NoMaDS is extending IACOB towards fainter magnitudes using the 9 m Hobby-Eberly Telescope (Maíz Apellániz et al. 2012; Pellerin et al. 2012). Finally, CAFÉ-BEANS is doing multi-epoch spectroscopy of northern stars to study their spectroscopic binarity (Negueruela et al. 2015). Combining those four high-resolution surveys,  $\sim 450$  O stars and another  $\sim 450$  early-type stars have been observed so far.

## 2. Dust: amount and type

We have recently derived a new family of optical+NIR extinction laws based on 30 Doradus data (Maíz Apellániz et al. 2014a). In

that paper we used a small data set to check its validity for Galactic sightlines. Our first goal here is to extend that verification to the larger data set of 448 Galactic O stars of the first two GOSSS survey papers (GOSSS I+II, Sota et al. 2011, 2014). For that purpose we have used the Galactic O-Star Catalog (GOSC, Maíz Apellániz et al. 2004; Sota et al. 2008 to collect Johnson  $UBV$  and 2MASS  $JHK_s$  photometry for all of the stars in the sample (after merging some unresolved binary systems) and Tycho-2  $BV$  and Strömgren  $uvby$  photometry in the cases where they were available. The photometry was processed using CHORIZOS (Maíz Apellániz 2004, 2013b) to obtain the amount  $[E(4405 - 5495)]$  and type  $[R_{5495}]$  of extinction (see Maíz Apellániz 2013a for an explanation of the choice of those quantities) in an analogous way to that used by e.g. Arias et al. (2006) or Maíz Apellániz et al. (2014a). Note that this procedure can be carried out with high precision due to the use of the  $T_{\text{eff}}$  derived from the GOSSS spectral types.

The CHORIZOS experiments were executed three times using the F99 (Fitzpatrick 1999), CCM (Cardelli et al. 1989), and M14 (Maíz Apellániz et al. 2014a) to test which of those families of extinction laws yields better fits to Galactic extinction. The  $\chi_{\text{red}}^2$  values (expected to be  $\sim 1$  in the ideal case) are shown in Fig. 1:

- The F99 results yield, on average, the poorest fits. Although they are not bad for low values of  $E(4405 - 5495)$  and  $R_{5495}$ , they worsen when either of those quantities increase (they are significantly bad for  $R_{5495} > 4$ ).
- The CCM results are better than those of F99 in terms of  $\chi_{\text{red}}^2$ . However, they yield poor results when Strömgren photometry is used due to their use of a seventh degree polynomial for interpolating in wavelength (F99 and M14 use splines, see Maíz Apellániz 2013a).
- The M14 results are the best of the three families. Indeed, the only case with  $\chi_{\text{red}}^2 > 3$  corresponds to an Oe star, which are expected to yield poor fits in some cases

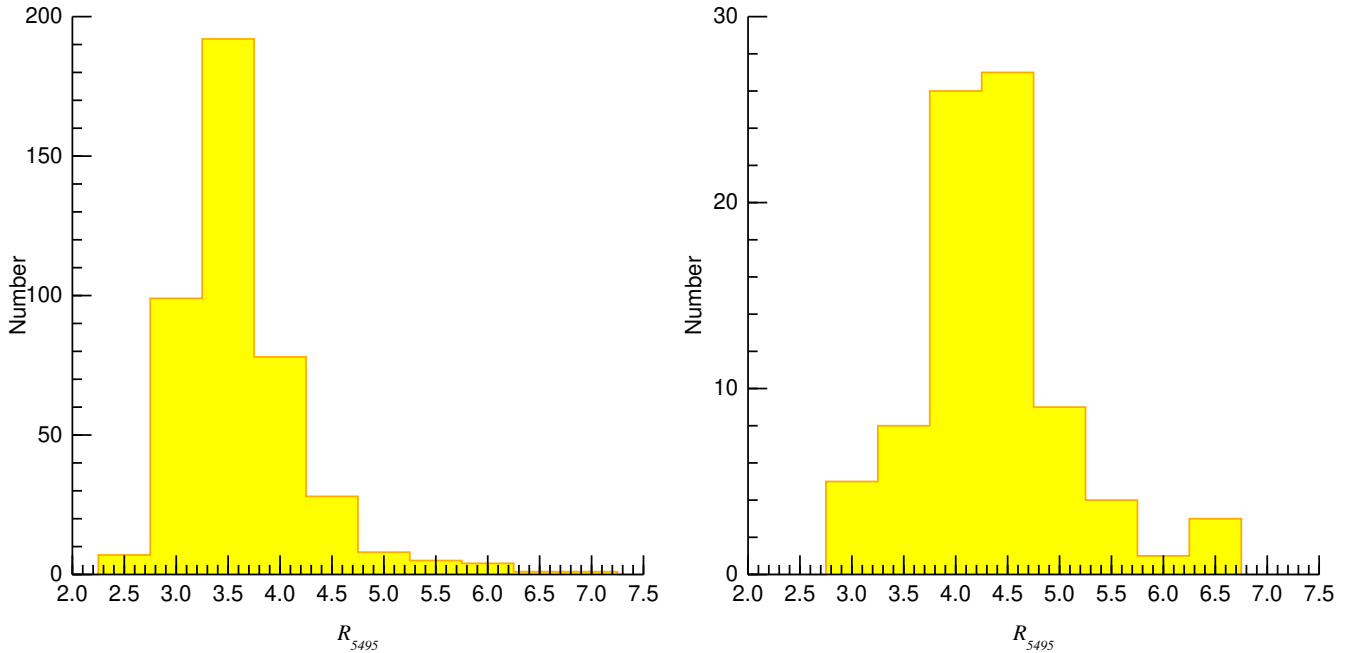


**Fig. 3.**  $R_{5495}$  histograms for the (Galactic) GOSSS I+II [left] and (30 Doradus) VFTS [right] samples.

due to the IR excesses produced by their disks. Therefore, the M14 family is the best choice for optical+NIR extinction not only in 30 Doradus but also in the Milky Way.

After choosing the M14 family, I show its detailed CHORIZOS results in Figs. 2 and 3. The latter also includes an  $R_{5495}$  histogram for the VFTS O-star sample in 30 Doradus (Evans et al. 2011; Maíz Apellániz et al. 2014a). The main findings are:

- As previously known for many decades, the majority of sightlines have  $R_{5495}$  between 3.0 and 3.5.
- At very low extinctions ( $E(4405 - 5495) < 0.2$ ) the error bars on  $R_{5495}$  are too large to yield significant results.
- There are few stars with  $R_{5495} < 3.0$  (sightlines with a large proportion of small dust grains) but they are a significant fraction of the objects with large extinction.
- In the range  $0.2 < E(4405 - 5495) < 1.2$  there is a significant fraction of stars with large values of  $R_{5495}$ . These sightlines are

depleted in small grains and are associated with H II regions.

- As previously noted, some Oe stars have a poor fit due to their IR excesses.
- The  $R_{5495}$  histograms for the Galaxy and 30 Doradus are markedly different, with the latter showing a larger fraction of high- $R_{5495}$  sightlines. The differences can be explained by [a] the lower values of  $E(4405 - 5495)$  and [b] the larger fraction of H II region sightlines in 30 Doradus.

In the future we plan to extend the analysis to the rest of the GOSSS sample, which is on average more extinguished than the one in this work.

### 3. DIBs

Another line of research using these O-star surveys is the study of the Diffuse Interstellar Bands (DIBs). Our long-term plans include the analysis of several tens of DIBs but here I concentrate on three of them: the 5780 and 5797 DIBs (central wavelengths of

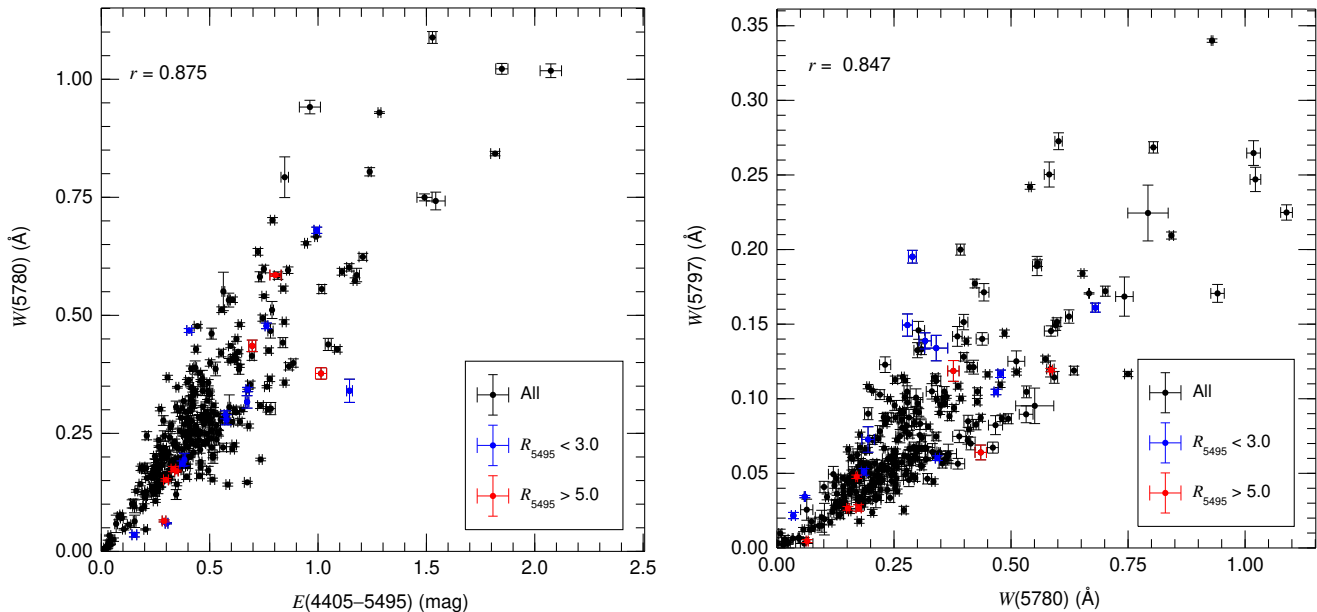


**Fig. 4.** [left]  $W(5780)$  as a function of  $E(4405 - 5495)$  and [right]  $W(5797)$  as a function of  $W(5780)$  for the GOSSS sample.

5780.48 Å and 5797.06 Å, respectively), which are among the most studied DIBs, and the 8621 DIB (central wavelength of 8620.65 Å), which is less studied but has received recent attention due to its inclusion in the wavelength region being observed by the Gaia RVS instrument.

We have extracted the equivalent widths ( $W$ ) for the three DIBs above using a subset of the high-resolution spectra in the surveys, correcting for saturation effects in the cases with deeper absorption profiles (this is not an issue for low values of extinction but some of our lines are heavily extinguished). These type of studies have been done before and the originality of this ongoing work lies in:

- The large sample in the survey, which in its final version will include over 1000 early-type star sightlines.
- The large dynamic range in extinction, which will eventually extend to  $A_V \sim 12$  (note that the subsample presented here only extends to  $A_V \sim 6$ ).

- The completeness down to a given magnitude (currently,  $B \sim 8$ , to be extended in the future) for O stars and the full-sky coverage.
- The use of modern values of  $E(4405 - 5495)$  and  $R_{5495}$  (see above) as extinction measurements.

I plot in Fig. 4  $W(5780)$  as a function of  $E(4405 - 5495)$  and  $W(5797)$  as a function of  $W(5780)$ . In both cases the two quantities are highly correlated but the Pearson correlation coefficient (shown in both plots) is between 0.8 and 0.9, a result similar to that of previous studies (e.g. Friedman et al. 2011; Vos et al. 2011; Raimond et al. 2012). More interestingly, in the right panel we can see that sightlines with low values of  $R_{5495}$  tend to lie above the average relationship while those with high values of  $R_{5495}$  tend to lie below the average relationship. To better visualize the effect, I plot in Fig. 5  $R_{5495}$  as a function of  $W(5797)/W(5780)$ . The Pearson correlation coefficient in that case is  $-0.384$ , significant but not very large.

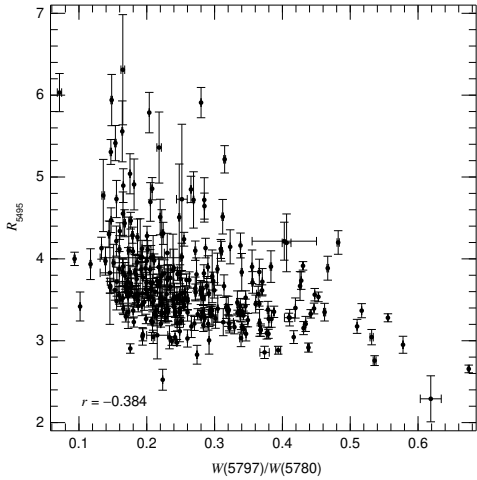


**Fig. 5.**  $R_{5495}$  as a function of  $W(5797)/W(5780)$  for the GOSSS sample.

However, the anticorrelation is clear when we examine the extremes of the distribution: all sightlines with  $W(5797)/W(5780) > 0.50$  have  $R_{5495} < 3.5$  and all with  $R_{5495} > 5.0$  have  $W(5797)/W(5780) < 0.35$ . Putting it in another way, most sightlines concentrate in the lower left quadrant of Fig. 5, with some points in the lower right and upper left quadrants and none in the upper right.

How do we interpret this result? It has been known for some time (Krelowski et al. 1997; Cox et al. 2005) that DIBs come in families and that the 5780 and 5797 DIBs are representative of two types of environments. The 5797 DIB is (relatively) strong in  $\zeta$  Oph, a sightline known to be exposed to a low UV flux, and is thus termed a “ $\zeta$  DIB”. On the other hand, the 5780 DIB is strong in  $\sigma$  Sco, a sightline exposed to a high UV flux, and is thus termed a “ $\sigma$  DIB”. See Fig. 6 and notice the large difference in the 5780 DIB for those two sightlines, which have a similar  $E(4405 - 5495)$ .  $\zeta$  Oph and  $\sigma$  Sco are the two prototypical examples of this phenomenon but in our sample we have found even more extreme cases such as HD 207 538 and  $\theta$  Mus B, also in Fig. 6. What we have found is that  $\zeta$  clouds (those with low UV flux) tend to have low values of  $R_{5495}$  (i.e. a larger proportion of small dust

grains) while  $\sigma$  clouds (those with high UV flux) tend to have large values of  $R_{5495}$  (i.e. a smaller proportion of small dust grains). Such a relationship between cloud type and  $R_{5495}$  was proposed by Cami et al. (1997), indicating that  $\zeta$  clouds likely correspond to cloud cores and  $\sigma$  clouds to cloud skins, but here we demonstrate its existence with a large sightline sample for the first time.

The difference in grain population between denser, non-UV-exposed,  $\zeta$  clouds and thinner, UV-exposed,  $\sigma$  clouds can be interpreted in terms of selective destruction of small grains in the latter. One interpretation would be that sputtering dominates over shattering in H II regions and other parts of the ISM exposed to UV light, as the former preferentially destroys small grains and the latter preferentially destroys large grains (Jones et al. 1994; Andersen et al. 2011). However, sputtering is only expected to become efficient above  $10^5$  K for refractory grains (Fig. 25.4 in Draine 2011), so a different mechanism is required. A possibility is that the extreme UV radiation present in H II regions destroys the PAHs that likely constitute the small grain population (Tielens 2008).

I also show in Fig. 7  $W(8621)$  as a function of  $E(4405 - 5495)$ . As expected, both quantities are strongly correlated with Pearson coefficients similar to those of other DIBs. Such measurements had been carried out before for that DIB but reaching lower values of  $E(4405 - 5495)$  (Munari et al. 2008; Kos et al. 2013). In the future we will extend this study to even larger extinctions.

#### 4. Individual sightlines

A third line of work is the study of individual sightlines in detail, of which we are analyzing several. Here we present a summary of our results on Berkeley 90, a little-studied cluster that includes two early-O-type systems, LS III +46 11 and LS III +46 12, separated by a short distance (Maíz Apellániz et al. 2015b).

Both stars show large extinctions but LS III +46 11 is significantly more extinguished than LS III +46 12 (by 30%).  $R_{5495}$ , on the other hand is very similar for both stars and

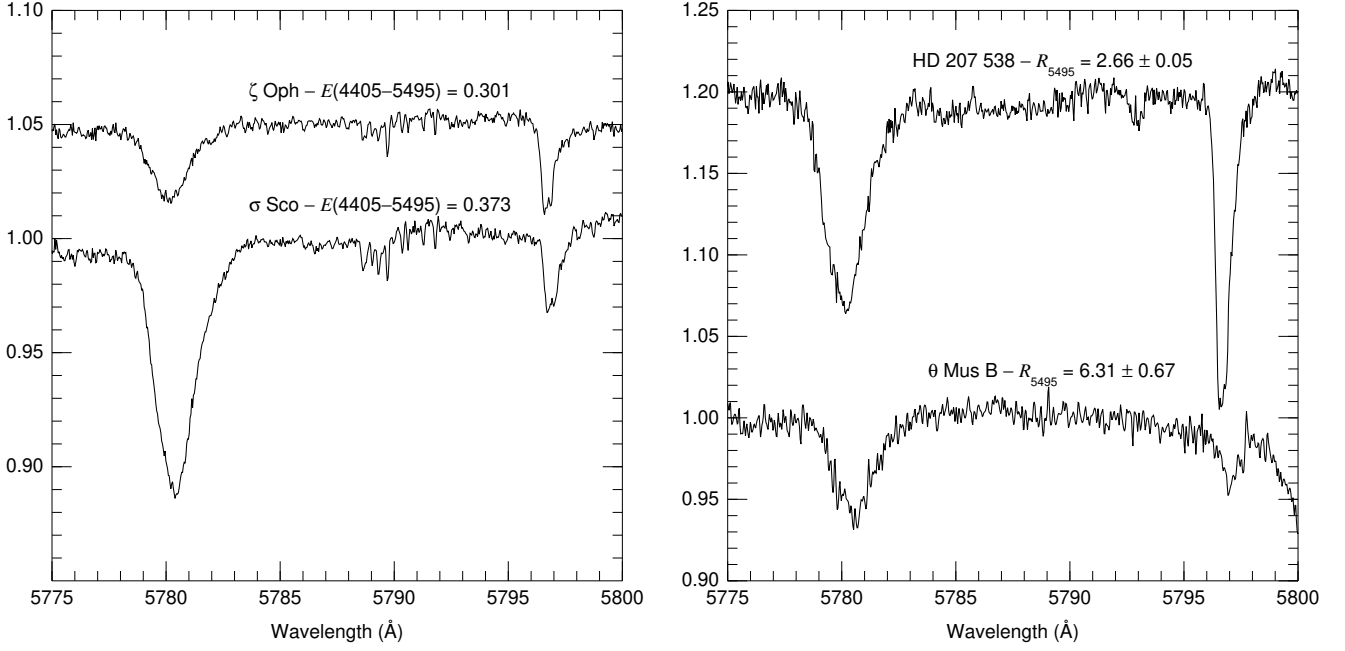


**Fig. 6.** [left] The prototype  $\zeta$  ( $\zeta$  Oph) and  $\sigma$  ( $\sigma$  Sco) sightlines for the 5780 and 5797 DIBs and [right] two more extreme examples, HD 207 538 ( $\zeta$ ) and  $\theta$  Mus B ( $\sigma$ ).

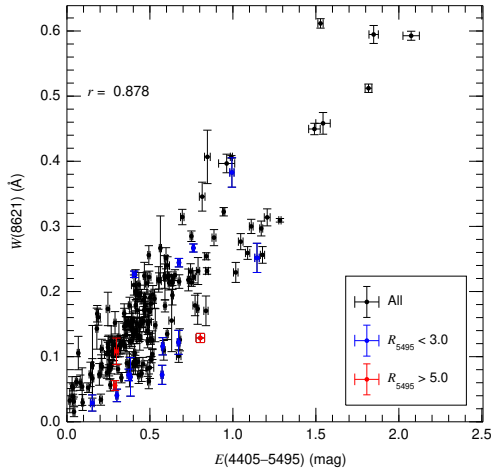


**Fig. 7.**  $W(8621)$  as a function of  $E(4405 - 5495)$  for the GOSSS sample.

has standard values between 3.3 and 3.4. We have measured as many as seven atomic, seven molecular, and fifty DIBs for both stars and

we have found large differences among them. We show in Fig. 8 the equivalent-width ratios for the lines we have measured. From the kinematic point of view, there are two components clearly visible in our high-resolution spectra. The weak one has a velocity intermediate between that of the cluster and ours, appears to be of relatively low density, and affects the two stars similarly. The strong one has a velocity similar to that of the cluster and affects the two stars differently: for LS III +46 12 it appears to be of lower density than for LS III +46 11. Combining all the information, we propose a model in which three different “clouds” (actually, one simple cloud and one cloud with core and skin) are located between Berkeley 90 and us (Fig. 9). The reader interested in more details is referred to Maíz Apellániz et al. (2015a).

One interesting result of the Berkeley 90 analysis is that it allows us to classify a large number of DIBs in a  $\sigma - \zeta$  scale, something that was not possible before due to the lack of

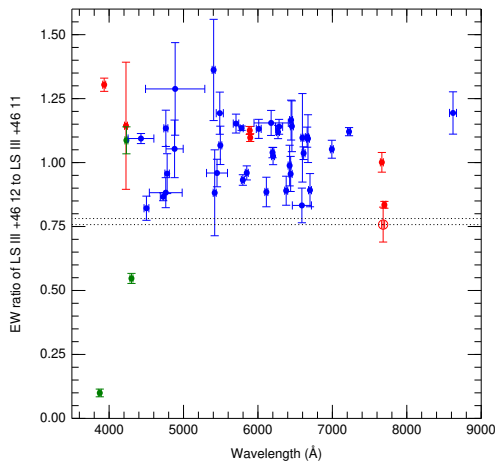


**Fig. 8.** Equivalent-width ratios between LS III +46 12 and LS III +46 11. Red is used for atomic lines, green for molecular lines, and blue for DIBs. All points show the EW uncorrected for saturation (which should be a good approximation in all cases except for the intense atomic lines) except for K I  $\lambda$ 7664.911+7698.974. In that case, besides the uncorrected values we show the corrected one (as an unfilled symbol) calculated using a kinematic decomposition. The  $x$  value in each case is  $\lambda_0$ , the length of the horizontal error bars is proportional (with a threshold for the narrowest ones) to the FWHM of the line, and the vertical error bars show the uncertainty in the measurement. The two dotted lines are the ratios for  $E(4405 - 5495)$  and  $A_V$ .

good data. In that sense, the 8621 DIB appears to be of  $\sigma$  type i.e. it samples the diffuse, UV-exposed ISM but not the dense, UV-shielded ISM.

The two sightlines have different values of  $W(5797)/W(5780)$  (0.34 and 0.28 for LS III +46 11 and LS III +46 12, respectively) but similar values of  $R_{5495}$ , which is in apparent contradiction with the correlation between  $W(5797)/W(5780)$  and  $R_{5495}$  previously discussed. However, that correlation is determined mostly by the extremes (sightlines with large values of  $R_{5495}$  and sightlines with large values of  $W(5797)/W(5780)$ ), which is the reason why the Pearson coefficient is not very large. For intermediate values Fig. 5

shows that it is possible to have variations in  $W(5797)/W(5780)$  without changing  $R_{5495}$ . In other words, the DIB-carrier population seems to change continuously with UV-field strength/density while for  $R_{5495}$  the variation seems to happen mostly at the extremes of the distribution (in H II regions and in very dense clouds), with an intermediate “typical” range where  $R_{5495}$  is nearly constant.

## 5. Conclusions

- The M14 family of extinction laws provides better optical+NIR fits than either F99 or CCM for both the Milky Way and 30 Doradus.
- $R_{5495}$  and  $W(5797)/W(5780)$  are anticorrelated, indicating that extreme  $\zeta$  clouds have a larger fraction of small dust grains than extreme  $\sigma$  clouds. However, in the intermediate region between the extremes it is possible to have clouds with the same grain distribution but different proportions of  $\zeta$  and  $\sigma$  DIBs.
- The 8621 DIB is strongly correlated with  $E(4405 - 5495)$  up to  $A_V \sim 6$  and the preliminary evidence for some sightlines point towards a  $\sigma$  character.

*Acknowledgements.* I thank my collaborators who participate in these surveys and M. Penadés Ordaz, who performed an initial reduction of the DIB data. I also thank Bruce Draine and Jacco van Loon for useful discussions on the relationship between  $R_{5495}$  and DIB types and Rodolfo Xeneize Barbá for general discussion on the ISM and for ideas and material that helped me understand this topic better. I acknowledge support from [a] the Spanish Government Ministerio de Economía y Competitividad (MINECO) through grants AYA2010-15 081, AYA2010-17 631, and AYA2013-40 611-P; [b] the Consejería de Educación of the Junta de Andalucía through grant P08-TIC-4075; and [c] the George P. and Cynthia Woods Mitchell Institute for Fundamental Physics and Astronomy. I am grateful to the Department of Physics and Astronomy at Texas A&M University for their hospitality during some of the time this work was carried out.



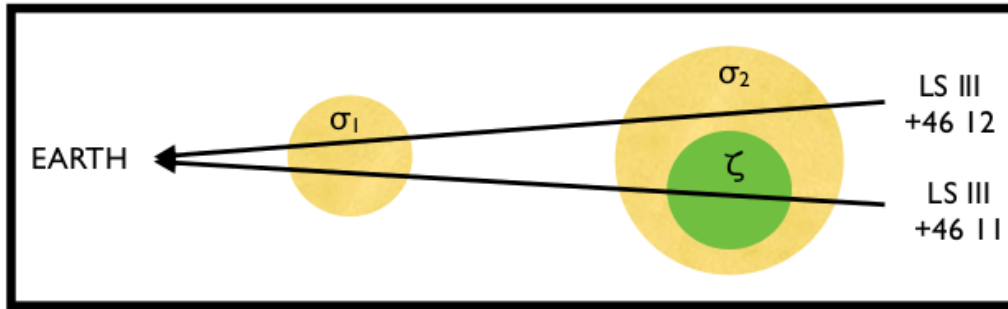


**Fig. 9.** Model for the ISM clouds present in the LS III +46 11 and LS III +46 12 sightlines. Cloud  $\sigma_1$  is of low density, not associated with the cluster, and affects both sightlines similarly. Cloud  $\sigma_2$  is also of low density, is the skin of the cloud associated with the cluster, and is longer along the LS III +46 12 sightline. Cloud  $\zeta$  is of high density, is the core of the cloud associated with the cluster, and affects LS III +46 11 exclusively (or, at least, to a much larger degree than LS III +46 12).

## References

- Andersen, M., Rho, J., Reach, W. T., Hewitt, J. W., & Bernard, J. P. 2011, *ApJ*, 742, 7
- Arias, J. I., Barbá, R. H., Maíz Apellániz, J., Morrell, N. I., & Rubio, M. 2006, *MNRAS*, 366, 739
- Barbá, R. H., Gamen, R. C., Arias, J. I., et al. 2010, in *Rev. Mex. Astron. Astrofís. (conference series)*, Vol. 38, 30–32
- Cami, J., Sonnentrucker, P., Ehrenfreund, P., & Foing, B. H. 1997, *A&A*, 326, 822
- Cardelli, J. A., Clayton, G. C., & Mathis, J. S. 1989, *ApJ*, 345, 245
- Cox, N. L. J., Kaper, L., Foing, B. H., & Ehrenfreund, P. 2005, *A&A*, 438, 187
- Draine, B. T. 2011, *Physics of the Interstellar and Intergalactic Medium* (Princeton University Press)
- Evans, C. J., Taylor, W. D., Hénault-Brunet, V., et al. 2011, *A&A*, 530, A108
- Fitzpatrick, E. L. 1999, *PASP*, 111, 63
- Friedman, S. D., York, D. G., McCall, B. J., et al. 2011, *ApJ*, 727, 33
- Jones, A. P., Tielens, A. G. G. M., Hollenbach, D. J., & McKee, C. F. 1994, *ApJ*, 433, 797
- Kos, J., Zwitter, T., Grebel, E. K., et al. 2013, *ApJ*, 778, 86
- Krelowski, J., Schmidt, M., & Snow, T. P. 1997, *PASP*, 109, 1135
- Maíz Apellániz, J. 2004, *PASP*, 116, 859
- Maíz Apellániz, J. 2013a, in *Highlights of Spanish Astrophysics VII*, 583–589
- Maíz Apellániz, J. 2013b, in *Highlights of Spanish Astrophysics VII*, 657–657
- Maíz Apellániz, J., Barbá, R. H., Sota, A., & Simón-Díaz, S. 2015a, *A&A*, submitted, arXiv:1508.07193
- Maíz Apellániz, J., Evans, C. J., Barbá, R. H., et al. 2014a, *A&A*, 564, A63
- Maíz Apellániz, J., Negueruela, I., Barbá, R. H., et al. 2015b, *A&A*, 579, A108
- Maíz Apellániz, J., Pellerin, A., Barbá, R. H., et al. 2012, in *Astronomical Society of the Pacific Conference Series*, Vol. 465, *Astronomical Society of the Pacific Conference Series*, ed. L. Drissen, C. Robert, N. St-Louis, & A. F. J. Moffat, 484
- Maíz Apellániz, J., Sota, A., Barbá, R. H., et al. 2014b, in *IAU Symposium*, Vol. 297, *IAU Symposium*, ed. J. Cami & N. L. J. Cox, 117–120
- Maíz Apellániz, J., Sota, A., Walborn, N. R., et al. 2011, in *Highlights of Spanish Astrophysics VI*, ed. M. R. Zapatero Osorio, J. Gorgas, J. Maíz Apellániz, J. R. Pardo, & A. Gil de Paz, 467–472
- Maíz Apellániz, J., Walborn, N. R., Galué, H. Á., & Wei, L. H. 2004, *ApJS*, 151, 103
- Munari, U., Tomasella, L., Fiorucci, M., et al. 2008, *A&A*, 488, 969
- Negueruela, I., Maíz-Apellániz, J., Simón-Díaz, S., et al. 2015, in *Highlights of Spanish Astrophysics VIII*, ed. A. J.

- Cenarro, F., Figueras, C., Hernández-Monteagudo, J., Trujillo Bueno, & L. Valdivielso, 524–529
- Pellerin, A., Maíz Apellániz, J., Simón-Díaz, S., & Barbá, R. H. 2012, in *American Astronomical Society Meeting Abstracts*, Vol. 219, American Astronomical Society Meeting Abstracts #219, 224.03
- Penadés Ordaz, M., Maíz Apellániz, J., & Sota, A. 2013, in *Highlights of Spanish Astrophysics VII*, ed. J. C. Guirado, L. M. Lara, V. Quilis, & J. Gorgas, 600–605
- Raimond, S., Lallement, R., Vergely, J. L., Babusiaux, C., & Eyer, L. 2012, *A&A*, 544, A136
- Simón-Díaz, S., Castro, N., García, M., & Herrero, A. 2011, in *IAU Symposium*, Vol. 272, IAU Symposium, ed. C. Neiner, G. Wade, G. Meynet, & G. Peters, 310–312
- Sota, A., Maíz Apellániz, J., Morrell, N. I., et al. 2014, *ApJS*, 211, 10
- Sota, A., Maíz Apellániz, J., Walborn, N. R., et al. 2011, *ApJS*, 193, 24
- Sota, A., Maíz Apellániz, J., Walborn, N. R., & Shida, R. Y. 2008, in *Rev. Mex. Astron. Astrofís. (conference series)*, Vol. 33, 56
- Tielens, A. G. G. M. 2008, *ARA&A*, 46, 289
- Vos, D. A. I., Cox, N. L. J., Kaper, L., Spaans, M., & Ehrenfreund, P. 2011, *A&A*, 533, A129
- Walborn, N. R., Maíz Apellániz, J., Sota, A., et al. 2011, *AJ*, 142, 150
- Walborn, N. R., Sota, A., Maíz Apellániz, J., et al. 2010, *ApJL*, 711, L143